Cell Tissue Bank (2015) 16:47–53
DOI 10.1007/s10561-013-9413-x

ORIGINAL PAPER

Dependence of optical attenuation coefficient and mechanical tension of irradiated human cartilage measured by optical coherence tomography

A. C. Martinho Junior · A. Z. Freitas · M. P. Raele · S. P. Santin · F. A. N. Soares · M. R. Herson · M. B. Mathor

Received: 24 May 2013 / Accepted: 23 November 2013 / Published online: 10 December 2013

Abstract As banked human tissues are not widely available, the development of new non-destructive and contactless techniques to evaluate the quality of allografts before distribution for transplantation is very important. Also, tissues will be processed accordingly to standard procedures and to minimize disease transmission most tissue banks will include a decontamination or sterilization step such as ionizing radiation. In this work, we present a new method to evaluate the internal structure of frozen or glycerol-processed human cartilages, submitted to various dosis of irradiation, using the total optical attenuation coefficient retrieved from optical coherence tomography (OCT) images. Our results show a close relationship between tensile properties and the total optical attenuation coefficient of cartilages. Therefore, OCT associated with the total optical attenuation coefficient open a new window to evaluate quantitatively biological changes in processed tissues.

Keywords Cartilage · Biomechanical · Optical coherence tomography

A. C. Martinho Junior · A. Z. Freitas (✉) · M. P. Raele · S. P. Santin · F. A. N. Soares · M. B. Mathor
Instituto de Pesquisas Energéticas e Nucleares (Ipen/CNEN-SP), São Paulo, Brazil
e-mail: freitas.az@ipen.br

M. R. Herson
The Alfred Skin Cell Culture Laboratory, Monash University, Melbourne, Australia

Introduction

The traditional methods to evaluate the quality of muscle-skeletal allografts processed in tissue banks involve sampling for microscopy and mechanical tests. These are destructive techniques that cause unnecessary loss of tissue, which could otherwise be transplanted. Donated human tissues are a precious gift; hence, the development of non-destructive techniques to evaluate the allografts before distribution for transplantation can be an important contribution for tissue banking.

Over the last decade, attention to optical coherence tomography (OCT) has been increased mainly in ophthalmology; however, other medical fields as orthopaedic surgery, cardiology, rheumatology, neurology, oncology and dermatology have been using OCT in several investigations. The successful use of OCT in medicine is due to its real time, high resolution imaging capacity of deep tissue structures in vivo, and because it is a contactless and non-destructive technique (Freitas et al. 2010; Wiesauer et al. 2006; Fujimoto 2002).

Optical coherence tomography (OCT) has been used to identify early osteoarthritis with good results (Xie et al. 2006; Roberts et al. 2003; Herrmann et al. 1999). OCT has also been used to characterize engineered tissues (Mason et al. 2004; Matcher 2011; Veksler et al. 2008). Moreover, OCT has been used following laser reshaping of spinal discs (Sobol et al. 2007) and nasal septum cartilage (Sobol et al. 2009) to evaluate postoperative changes in tissue.

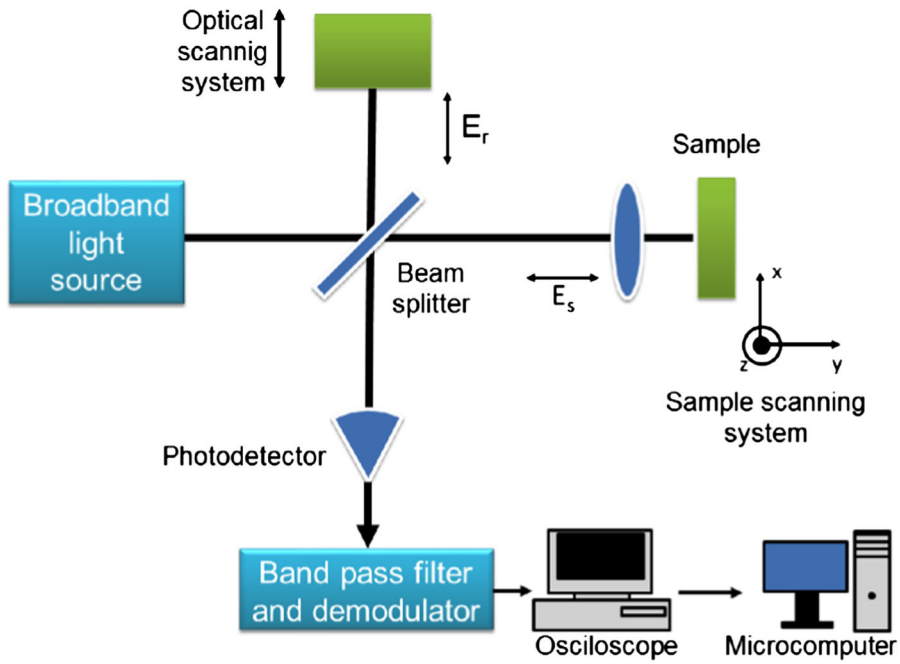

Fig. 1 Main components of the OCT setup

Analogous to ultrasound, OCT measures the backscattering intensity of infrared laser rather than sound. Backscattering intensity cannot be measured directly due to the high speed of the light; therefore OCT deploys a technique known as low coherence interferometry. Although able to generate cross-sectional images (2-D) of tissues as in microscopy and ultrasonography, biological samples for OCT analysis do not require any prior preparation, preventing any undesirable changes in examined tissues (Brezinski 2006). Moreover, thin cross-sectional images may be used to recreate three-dimensional sample structures (Freitas et al. 2009).

Highly scattered composite structures remain as a limiting factor for OCT studies. New methods to decrease statistical noise associated with the multiple scattering have been developed for OCT (Buranachai et al. 2009) and for polarization-sensitive optical coherence tomography (PS-OCT) (Macdonald and Meglinski 2011). In this option, the broadband light in an OCT system is coupled into a fiber-optic Michelson interferometer and is divided in two light beams by a beam splitter. One beam is directed to a reference mirror that is precisely controlled by a computer and another light beam is directed to the sample. The light backscattered by the sample and the light reflected by the mirror are recombined at the beam splitter generating an interference pattern which is collected by the detector (Fig. 1) (Freitas et al. 2009, 2010).

Optical coherence tomography (OCT) comes to cover a gap left by other imaging techniques (Freitas et al. 2010). Despite having the deepest range, ultrasound does not generate high resolution images and confocal microscopy does not have high penetration into the tissue. OCT imaging will typically include a 2–3 mm depth associated with a high resolution images of 4–20 μm (Brezinski 2006; Brezinski et al. 1996; Huang et al. 1991).

Cartilage is an anisotropic material and is a specialized type of connective tissue which supports mechanical stress without undergoing permanent deformation (Veksler et al. 2008). This tissue is widely used for reconstructive surgeries of ear, nose, penis (Vajaradul 2000; Strauch and Wallach 2003), for thoracic reconstruction in children affected by Pectus Excavatum (Feng et al. 2001) and Poland's syndrome (Akal and Kara 2002). Water represents almost 80 % of total weight of this tissue and collagen type II corresponds for 30 % of dry weight (Hasler et al. 1999).

Until this moment, no publication has dealt with the potential contribution of OCT in Tissue Banking. In this work, we present a new method to evaluate the internal structure of post-processed human cartilage, using the total optical attenuation coefficient retrieved from OCT images.

Materials and methods

Material processing

This work was approved by the Ethics Committee of the Faculdade de Saúde Pública of the Universidade de São Paulo. Forty paired and symmetric fragments of costal cartilages were obtained from twenty cadaver donors (aged from 18 to 45 years), both male and female. The right costal cartilages were snap frozen at −70 °C (Vajaradul 2000; Komender et al. 2001) and the left costal cartilages were preserved in high concentration of glycerol (85 %) (Herson and Mathor 2006). The 20 frozen or glycerolized samples were divided in four experimental groups (n = 5). One group was identified as Control Group (i.e. non-irradiated) and the other three were irradiated by a ^{60}Co source with doses of 15, 25 or 50 kGy. During irradiation, the Control Group samples were kept in the same environmental conditions as the experimental groups. In particular, to avoid significant environmental temperature variations, frozen cartilages were irradiated in the presence of dry-ice, while glycerolized cartilages were irradiated in the presence of cooling blocks. Red Perspex dosimeters were used as dose control.

Before further testing, glycerolized cartilages were rehydrated in saline solution (0.9 % NaCl) and frozen cartilages were thawed at room temperature.

OCT

Optical coherence tomography images of costal cartilages were obtained from OCP930SR (Thorlabs, USA) with spatial resolution of 6 microns and optical power of 2 mW in the sample. The samples were previously thawed and rehydrated as described above. Five OCT images were taken from each sample, generating 200 OCT images. Each image was analyzed by homemade software designed to calculate the total optical attenuation coefficient, as described in the next topic.

Total optical attenuation coefficient

A homesoftware was developed to retrieve the total optical attenuation coefficient from OCT signal. At first, all OCT scans in region of interest selected by user (ROI) were aligned in consideration of the surface curvature, then an average OCT signal (vertical lines in the OCT image) were generated calculating the arithmetic median. Figure 2 shows the frontend of developed software, where the vertical bars in the upper picture defines the ROI, the inset shows the ROI selected and the graph in the lower picture show the averaged OCT signal and its fitted corresponding function. The user can select another ROI in the OCT averaged signal, initiating some microns below the sample surface and some microns before the sample end (in the image). This is done by selecting the appropriated range in software interface. The user can also choose starts some percentage value of signal decay, but in our analysis it was not used.

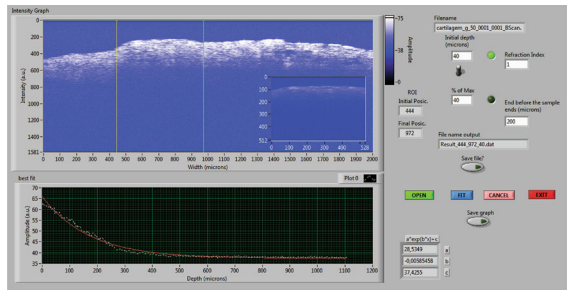

Fig. 2 The frontend of developed software in LabVIEW 8.0 (National Instruments academic license), the *vertical bars* on the *upper part* of figure defines de ROI, the *inset* shows the ROI selected by user and the graph on the *lower part* of figure shows the averaged OCT signal and its corresponding function fitted. On the *right side* are showed all parameter that user can set (see description in the text)

To determine the appropriated ROI, a previous study was done and the best common range, for all samples, was used to calculate the total optical attenuation coefficient. After the user selects the predefined ROI, the program performed an exponential fit using the function:

$$f(x) = a \exp(-2\ b\ x) + c$$

where "a" is the amplitude of backscattering signal in the surface, "b" is the total optical attenuation coefficient inside the sample and "c" is a background level due to signal noise.

Biomechanical tests

The biomechanical testing in tension was immediately followed the OCT analysis. To perform the mechanical tests, 2 mm thickness samples were obtained from

the superficial zone of the cartilages deemed responsible for tensile properties (Hunziker et al. 1997) and were cut into dumbbell shapes as shown in Fig. 3 (Martinho Junior et al. 2013).

The tests were carried out on a universal tensile testing machine (Instron, model 5567, MA, USA) with 1 kN load module, 10 mm distance between grips and the cross-head set to move at 5 mm/min until failure. A rough surface in the static and moving grips was used to avoid run off of the samples, which were mechanically locked in the jaws. The stress–strain curve was recorded automatically.

Statistical analysis

One-way ANOVA test ($p < 0.05$) was used to look for significant differences between control and experimental groups. Results were expressed as mean value with its uncertainty in figures.

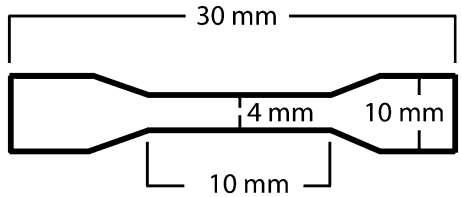

Fig. 3 Dimensions of samples in dumbbell cut

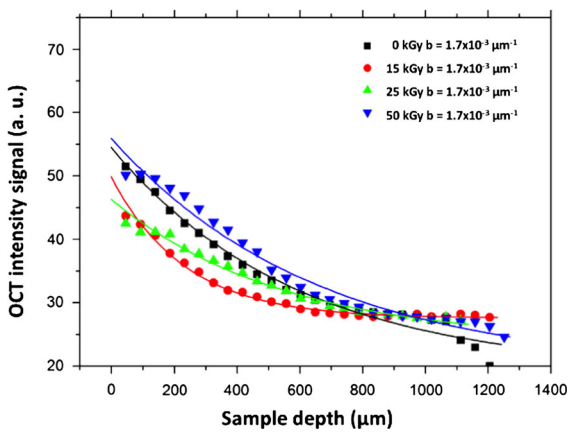

Fig. 4 The OCT signal and its exponential decay fits for frozen cartilages and irradiated with different doses, where can be observed the total optical attenuation coefficient variation (parameter *b*), as discussed in the text

Results

Some OCT signal (e.g.) obtained from frozen cartilages and irradiated with different doses are showed in Fig. 4.

For all samples, mechanic failure occurred between the jaws. Figures 5 and 6 illustrate the correlation between the biomechanical tension property and the total attenuation coefficient of photons derived from the OCT signal, within the specific processing method. On these images, we find a correlation between mechanical and photonics cartilage properties. For the dose of 15 kGy, an increase in both stress at break and total optical attenuation coefficient were observed. However, when cartilages are irradiated with 25 or

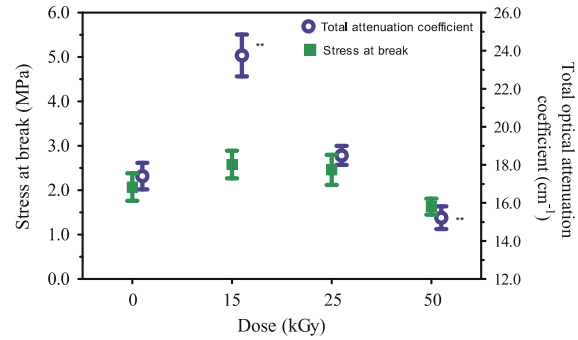

Fig. 5 Correlation between stress at break and total optical attenuation coefficient in frozen cartilages. The symbol ** was used to show data with statistical significance ($p < 0.05$) for total optical attenuation coefficient in relation to its respective control group

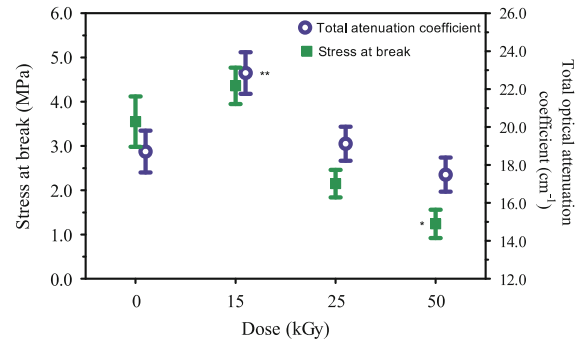

Fig. 6 Correlation between stress at break and total optical attenuation coefficient in glycerol-processed cartilages. The symbol * was used to show data with statistical significance ($p < 0.05$) for stress at break; and ** for total optical attenuation coefficient ($p < 0.05$) in relation to its respective control group

50 kGy, both stress at break and total optical attenuation coefficient decreased proportionally to the dose.

Discussion

To reduce risk in disease transmission through allografts, most Tissue Banks will deploy some kind of sterilization method of grafts before distribution for transplantation. Ionizing radiation is a widespread option used to sterilize allografts as it has high penetration in matter without significant variations on the temperature. Moreover, tissues can be sterilized by ionizing radiation in their final packaging, thus avoiding exposure to new contaminants. Nevertheless, high doses of ionizing radiation may cause undesirable changes on the allografts, changing their mechanical properties due to the degradation of the structural scaffold with increased in vivo resorption rates (Dziedzic-Goclawska 2000).

The evolving OCT techniques have allowed for a considerable advance in the understanding of cartilage ultrastructure, allowing for the development of algorithms that calculate physical properties through the total optical attenuation coefficient (Fig. 4), making it possible not only to generate images without changes in tissue composition and properties due to use of fresh samples, but also to analyze and physically compare the biological changes occurred in tissues caused by innumerable reasons, such as those caused by ionizing radiation or by triggered by various diseases.

Few previous publications have dealt with the use of OCT and mechanical properties of biological tissue. Wave propagation in mouse crystalline lens, and describes a new method to evaluate mechanical properties of materials with high sensitivity. However, the relationship between optical properties and mechanical properties such as tensile strength are not discussed. Braz et al. (2009) investigates crack propagation in dental composites used in dental restorations and describes a method to visualize internal cracks caused by thermal and mechanical cycles; once again, no correlation between optical and mechanical properties is quantified.

In our work, as in Figs. 5 and 6, a relationship between cartilage stress at break and the total optical attenuation coefficient was identified. The irradiation dose of 15 kGy caused an increase in stress at break and in total optical attenuation coefficient, in both frozen and glycerolized cartilages. The increased image scattering suggests that this dose of irradiation promotes cross-links into collagen network with increased density, an event well known (Nguyen et al. 2007). These collagens cross-links can be visualized in picro-sirius staining histological sections (Martinho Junior 2012), corroborating the OCT evidences. The increase of total optical attenuation coefficient in frozen cartilages was not followed by a significant increase in stress at break as occurs for glycerolized cartilages and this fact is caused by preservation method and was discussed in more details in a previous work (Martinho Junior et al. 2013).

For doses of 25 and of 50 kGy there is a decrease of both stress at break and total optical attenuation coefficient. At these doses, ionizing radiation promotes more rupture in collagen fibrils than cross-linking, which may cause a decrease in the mechanical properties of the tissue (Nguyen et al. 2007). However, the changes in tissue structure did not affect the performance of the frozen allograft significantly, as there were no statistical differences ($p < 0.05$) between irradiated cartilages and control, when cartilages were frozen at -70 °C. On the other hand, glycerolized cartilages showed a significant decrease in stress at break when irradiated with doses of 50 kGy.

Our results for the total optical attenuation coefficient of cartilage were in accordance to those found by Cheong et al. (1999). When just total optical attenuation coefficient is taken into consideration, frozen cartilages irradiated with doses of 15 or 50 kGy presented a significant statistical differences ($p < 0.05$) to the Control Group. Only glycerolized cartilages that were irradiated with 15 kGy showed a statistical difference as far as the total optical attenuation coefficient. Furthermore, no significant statistical differences ($p < 0.05$) were found for same donor sample's indicating that ROI must be pre-defined to avoid greater variations in total optical attenuation coefficient among OCT images of the same sample as well as for all samples in study.

As the total optical attenuation coefficient seems to be directly associated with changes in tissue structure, the photonics properties of tissues could be used to estimate their mechanical properties more precisely. These findings suggest that OCT associated with total optical attenuation coefficient may be a more sensitive technique than mechanical tests to evaluate the changes in structure, and thus performance, of processed and irradiated cartilage.

Despite of mechanical tests remaining the a gold standard to evaluate the structure and performance of tissues, the use of the proposed technique has the advantage that tissue integrity, or sterility, may not be compromised, preventing loss of allografts that could otherwise be transplanted.

Conclusions

Optical coherence tomography (OCT) associated with total optical attenuation coefficient is an efficient method to evaluate performance-impacting changes in tissue structure caused by tissue processing and radiation sterilization.

This work opens a new scope for the use of OCT analysis to characterize, quantitatively, biological changes in tissues and can added value to the wide range of existing testing methods.

Acknowledgments We would acknowledge the International Atomic Energy Agency (IAEA), the Comissão Nacional de Energia Nuclear (CNEN), and the Fundação de Amparo à Pesquisa do Estado de São Paulo (Fapesp) (Grant No. 2008/10437-9) for supporting this work.

References

Akal M, Kara M (2002) The use of a homologous preserved costal cartilage in an infant with Poland's syndrome. Eur J Cardiothorac Surg 21:146–148

Braz AKS, Kyotokub BBC, Brazc R, Gomes ASL (2009) Evaluation of crack propagation in dental composites by optical coherence tomography. Dent Mater 25:74–79

Brezinski ME (2006) Optical coherence tomography: principles and applications. Academic Press, London

Brezinski ME, Tearney GJ, Bouma BE, Izatt JA, Hee MR, Swanson EA, Southern JF, Fugimoto JG (1996) Optical coherence tomography for optical biopsy: properties and demonstration of vascular pathology. Circulation 93(6): 1206–1213

Buranachai C, Thavarungkul P, Kanatharana P, Meglinski IV (2009) Application of wavelet analysis in optical coherence tomography for obscured pattern recognition. Laser Phys Lett 6(12):892–895

Cheong WF, Prahl SA, Welch AJ (1999) A review of the optical properties of biological tissues. IEEE J Quantum Electron 26:2166–2185

Dziedzic-Goclawska A (2000) The application of ionizing radiation to sterilize connective tissue allografts. In: Phillips GO (ed) Cell Tissue Bank 123 Author's personal copy. Radiation and tissue banking. World Scientific, UK

Feng J, Hu T, Liu W, Zhang S, Tang Y, Chen R, Jiang X, Wei F (2001) The biomechanical, morphologic, and histochemical properties of the costal cartilages in children with pectus excavatum. J Pediatr Surg 36(12):1770–1776

Freitas AZ, Zezell DM, Mayer MPA, Ribeiro AC, Gomes ASL, Vieira ND Jr (2009) Determination of dental decay rates with optical coherence tomography. Laser Phys 6(12):896–900

Freitas AZ, Magri MA, Raele MP (2010) Optical coherence tomography: development and applications. In: Duarte FJ (ed) Laser pulse phenomena and applications. InTech, Rijeka, pp 409–432

Fujimoto JG (2002) Optical coherence tomography: introduction. In: Bouma B, Tearney GJ (eds) Handbook of optical coherence tomography optical coherence tomography. Marcel Dekker, New York, pp 1–40

Hasler EM, Herzog W, Wu JZ, Müller W, Wyss U (1999) Articular cartilage biomechanics: theoretical models, material properties, and biosynthetic response. Crit Rev Biomed Eng 27(6):415–488

Herrmann JM, Pitris C, Bouma BE, Boppart SA, Jesser CA, Stamper DL, Fujimoto JG, Brezinski ME (1999) High resolution imaging of normal and osteoarthritic cartilage with optical coherence tomography. J Rheumatol 26(3):627–635

Herson MR, Mathor MB (2006) Bancos de Tecidos. In: Garcia VD, Abud M, Neumann J, Pestana JOM (eds) Transplantes de Órgãos e Tecidos, 2nd edn. Segmento Farma Editores Ltda, São Paulo, pp 174–185

Huang D, Swanson EA, Lin CP, Schuman JS, Stinson WG, Chang W, Hee MR, Flotte T, Gregory K, Puliafito CA, Fujimoto JG (1991) Optical coherence tomography. Science 254:1178–1181

Hunziker EB, Michel M, Studer D (1997) Ultrastructure of adult human articular cartilage matrix after cryotechnical processing. Microsc ResTech 37:271–284

Komender J, Marczynski W, Tylman D, Malczewska H, Komender A, Sladowski D (2001) Preserved tissue allograft in reconstructive surgery. Cell Tissue Bank 2:103–112

Macdonald C, Meglinski IV (2011) Backscattering of circular polarized light from a disperse random medium influenced by optical clearing. Laser Phys Lett 8(4):324–328

Martinho Junior AC (2012) Estudos dos efeitos da radiação ionizante em cartilage costal humana por meio de tomografia por coerência óptica e termogravimentria. Dissertation, University of São Paulo

Martinho Junior AC, Rosifini Alves-Claro AP, Pino ES, Machado LDB, Santin SP, Mathor MB (2013) Effects of ionizing radiation and preservation on biomechanical properties of human costal cartilage. Cell Tissue Bank 14(1):117–124

Mason C, Markusen JF, Town MA, Dunnill P, Wang RK (2004) The potential of optical coherence tomography in the engineering of living tissue. Phys Med Biol 49(7):1097–1115

Matcher SJ (2011) Practical aspects of OCT imaging in tissue engineering. Methods Mol Biol 695:261–280

Nguyen H, Morgan DAF, Forwood MR (2007) Sterilization of allograft bone: effects of gamma irradiation on allograft biology and biomechanics. Cell Tissue Bank 8:93–105

Roberts MJ, Adams SB, Patel NA, Stampler DL, Westmore MS, Martin SD (2003) A new approach for assessing early osteoarthritis in the rat. Anal Bioanal Chem 377:1003–1006

Sobol EN, Milner TE, Shekhter AB, Baum OI, Guller AE, Ignatieva NY, Omelchenko AI, Zakharkina OL (2007) Laser reshaping and regeneration of cartilage. Laser Phys Lett 4:488–502

Sobol EN, Zakharkina O, Baskov A, Shekhter A, Borschenko I, Guller A, Baskov V, Omelchenko A, Sviridov A (2009) Laser engineering of spine discs. Laser Phys 19:825–835

Strauch B, Wallach G (2003) Reconstruction with irradiated homograft costal cartilage. Plast Reconstr Surg 111(7): 2405–2411

Vajaradul Y (2000) Bangkok biomaterial center: 15 years experience in tissue banking. Cell Tissue Bank 1:229–239

Veksler B, Kobzev E, Bonesi M, Meglinski I (2008) Application of optical coherence tomography for imaging of scaffold structure and micro-flows characterization. Laser Phys Lett 5(3):236–239

Wiesauer K, Pircher M, Götzinger E, Hitzenberger CK, Engelke R, Ahrens G, Grützner G, Stifter D (2006) Transversal ultrahigh-resolution polarizationsensitive optical coherence tomography for strain mapping in materials. Opt Express 14(13):5945–5953

Xie T, Guo S, Zhang J, Chen Z, Peavy GM (2006) Determination of characteristics of degenerative joint disease using optical coherence tomography and polarization sensitive optical coherence tomography. Lasers Surg Med 38(9): 852–865